JOURNAL OF PROPULSION AND POWER
Vol. 12, No. 2, March–April 1996

# Simple Geometric Model for Estimating the Impingement Current on Ion Thruster Grids

W. M. Ruyten*
*Center for Space Transportation and Applied Research, Tullahoma, Tennessee 37388*

**A simple model is presented for estimating the magnitude and distribution of the impingement current on the accelerator grid of a two-grid ion thruster operating at a chamber pressure that is high enough that the chamber gas may be expected to be the dominant source of charge-exchange ions. The effective length over which these ions are redirected to the outer grid is shown to be in the range of 0.35–0.45 thruster radii for typical beam geometries. Model predictions are compared against experimental values for two widely different tests. For one of these it is argued that overprediction of the impingement current may be interpreted as circumstantial evidence for the existence of potential gradients that prevent chamber ions from backstreaming to the grid.**

## Nomenclature

$A, B, C$ = quantities defined in Eqs. (10)
$f_\Omega$ = solid-angle-probability factor
$J_b$ = total beam current
$J_i$ = impingement current
$J_z(r)$ = current density at axial position $z$
$\langle l_\Omega \rangle$ = charge-exchange length
$n_0$ = neutral density in plume
$P(\rho)$ = dimensionless beam profile
$q$ = ion charge
$R$ = ion beam radius at grid
$\dot{R}_{ce}$ = production rate of charge-exchange ions
$R_z$ = ion beam radius at axial position $z$
$r, z$ = cylindrical coordinates in plume
$s$ = radial coordinate in grid plane
$\gamma$ = divergence half-angle of ion beam
$\varepsilon$ = shape flatness parameter from Eq. (11)
$\rho$ = dimensionless radial coordinate in plume
$\sigma$ = dimensionless radial coordinate on grid
$\sigma_{ce}$ = charge-exchange cross section
$\varphi$ = azimuthal angle from Fig. 1

## I. Introduction

IT is well known that the production of charge-exchange (CE) ions is the principal grid-erosion mechanism in ion thrusters. If a CE ion is produced near the accelerator grid, it is likely to be drawn to this grid regardless of the magnitude and direction of its velocity. But, in two-grid thrusters, CE ions produced in the plume may also backstream to the accelerator grid if their velocity vectors point toward the grid. In ground testing of space thrusters, such backstreaming of CE ions from the plume may dominate the grid erosion process, depending on the pumping speed of the test facility. In this case, it is difficult to extrapolate grid lifetimes measured in the ground test to grid lifetimes for operation in space.

Particle-in-cell (PIC) simulation models are under development to aid in such extrapolations.[1–3] These models tend to be complex and computationally intensive. Moreover, they typically model only a single set of grid apertures. As a result, they are not very well suited to incorporate the effect of thruster size and they are forced to include the effect of grid diameter in an approximate manner. In the limit where backstreaming of CE ions from the plume becomes the dominant erosion mechanism, the results of the PIC calculation become almost entirely dependent on the choice of the downstream boundary conditions, which may be hard to specify a priori.[3]

To improve this situation, a simple model is developed here that can be used to estimate the contribution of CE ions from the plume to the impingement current on the accelerator grid of a two-grid system (a three-grid system is presumed to be operated in such a way that it repels CE ions from the plume). The model should be expected to give a lower bound for the impingement current on the accelerator grid, because it does not take into account the contributions from CE ions produced near the grid apertures (modeled so well with the PIC codes), nor of CE ions that are produced in charge-exchange collisions between the ion beam and neutral gas leaking from the thruster.

## II. Mathematical Model

The basic assumption of the model is that the probability that a CE ion from the plume will backstream to the outer thruster grid is given solely by the solid angle subtended by the grid as seen from the point where the CE ion is produced. Additional assumptions are as follows:

1) The ion beam may be treated as a single beam, rather than one which is comprised of a large number of discrete beamlets defined by individual apertures in the grid.

2) The trajectory of a CE ion from the plume may be approximated by a straight line. Thus, any curvature of the trajectory that results when the ion passes through the neutralization sheath is neglected. This approximation is justified a posteriori by the result that the effective charge-exchange length that follows from the model (somewhat less than half a thruster radius) is much larger than a typical value for the distance between the accelerator grid and the neutralization plane (typically on the order of one-tenth of a thruster radius[1,4]).

3) CE ions are not barred from backstreaming to the accelerator grid by positive potential hills in the individual beamlets that are extracted from the thruster (e.g., as described in Refs. 1 and 5). Any deflection close to the grid is presumed to be small enough that the CE ion still impacts on the grid.

4) The neutral density is constant throughout the plume and the distribution of velocity vectors of neutrals is isotropic. Note that the presence of additional neutral atoms that emanate di-

Received Aug. 14, 1993; revision received Feb. 28, 1995; accepted for publication Oct. 8, 1995. 

*Currently Senior Engineer, Instrumentation and Diagnostics Group, Sverdrup Technology, Inc., Arnold Engineering Development Center, Tullahoma, TN 37389-1300.

rectly from the thruster does not invalidate this assumption so much as point out that the calculated grid impingement current will be a lower bound.

5) The ion-neutral momentum transfer in a charge-exchange collision is negligible.[6] Thus, the isotropic distribution of velocities assumed in 4 is retained in the distribution of velocities of the CE ions. That is, CE ions are emitted in all directions with equal probability. (Actually, some momentum transfer does take place, thereby imparting a small velocity to the CE ion that is perpendicular to the velocity vector of the incident beam ion.[6])

Figure 1 defines the geometry of the problem: the cross section of the thruster, taken at the location of the accelerator grid, is assumed to be given by a circle of radius $R$. A point $P$ in the plume is located at a distance $z$ from the accelerator grid, displaced from the axis by a distance $r$. A point $Q$ on the grid is defined relative to $P$ by the polar coordinates $s$ and $\varphi$ in the thruster plane. With the previous assumptions, the probability that a CE ion emitted at $P$ should impact the grid at $Q$ is given by $1/(4\pi)$ times the solid angle subtended by the surface element $d^2A$ ($=s\,ds\,d\varphi$) surrounding $Q$. Integrating over all possible points $Q$ on the surface, the solid-angle-based probability that a CE ion produced at a point $(z, r)$ will impact on the grid becomes

$$f_\Omega(z, r) = \frac{1}{4\pi}\int_0^R s\,ds \int_0^{2\pi} d\varphi \frac{z}{(z^2 + r^2 + s^2 - 2rs\cos\varphi)^{3/2}} \tag{1}$$

The integrand in Eq. (1) is essentially the quantity $\cos\vartheta/a^2$, where $a$ is the distance between $P$ and $Q$ in Fig. 1, and $\vartheta$ is the angle of the line segment joining $P$ and $Q$ to the normal of the thruster surface. From Eq. (1) it is easy to calculate $f_\Omega$ for any point $(z, r)$ in the downstream region of the thruster: the integral over the radius $s$ can be performed analytically, leaving for numerical integration only the integral over the angle $\varphi$ (which, based on symmetry, only has to be carried out over half the range).

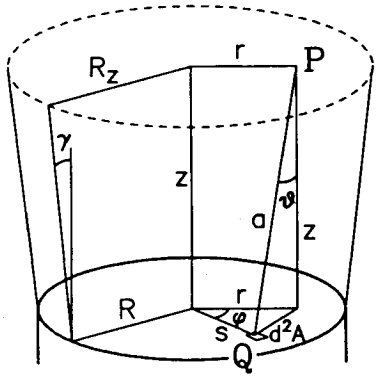


**Fig. 1 Assumed geometry of the ion source and the extracted beam. The accelerator grid is located at $z = 0$.**

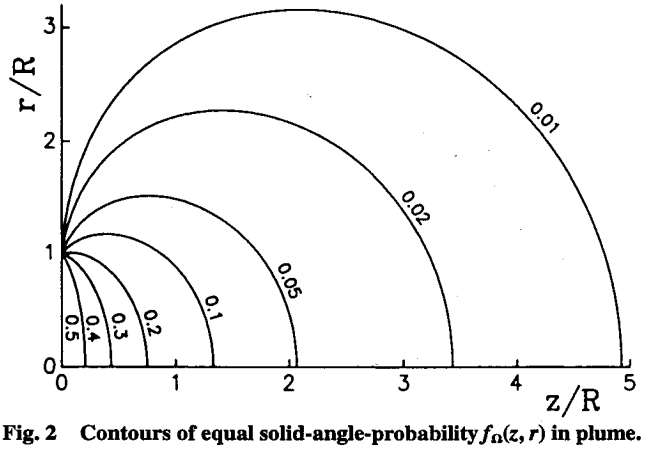


**Fig. 2 Contours of equal solid-angle-probability $f_\Omega(z, r)$ in plume.**

Figure 2 shows calculated equi-$f_\Omega$ contours. At the thruster surface ($r \leq R$; $z = 0$) the probability peaks at the value 0.5 (the CE ion is emitted, with equal probability, either toward the thruster or away from it) and drops off with increasing distance from the thruster. Points on the thruster edge ($r = R$; $z = 0$) are singular: all equi-$f_\Omega$ contours emanate from this edge, swelling up to roughly circular arcs far away from the thruster plane. (In two dimensions the loci of points that enclose a given line segment with equal angles are given by circular arcs exactly.) Not surprisingly, the geometric scale over which the solid-angle-probability drops to zero is on the order of one thruster diameter.

To calculate the impingement current that results from the backstreaming of CE ions, we must specify the current density distribution of beam ions in the plume. Denoting this distribution by $J_z(r)$, the total beam current $J_b$ becomes

$$J_b = \int_0^\infty J_z(r) r\,dr \tag{2}$$

For simplicity, it is assumed that depletion of the primary ion beam due to charge exchange may be neglected. This is justified by the observation that the mean free path for charge exchange is typically much larger than the charge-exchange length that follows from the model. As a result, the radially integrated beam current is $z$-independent, even though the radial profile may depend on the axial position $z$ due to beam divergence.

We can now write down an expression for the production rate of CE ions, at some point $(z, r)$:

$$\dot{R}_{ce}(z, r) = J_z(r) n_0 \sigma_{ce}/q \tag{3}$$

Integration over the downstream region now gives the impingement current on the grid as

$$J_i = q\int_0^\infty r\,dr \int_0^\infty dz\,\dot{R}_{ce}(z, r) f_\Omega(z, r) \tag{4}$$

By combining Eqs. (2–4), we can express the ratio of impingement and beam currents as

$$J_i/J_b = n_0 \sigma_{ce} \langle l_\Omega \rangle \tag{5}$$

where $\langle l_\Omega \rangle$ is an effective charge-exchange length given by

$$\langle l_\Omega \rangle = \iint r\,dr\,dz\,f_\Omega(z, r) J_z(r) \Big/ \int r\,dr J_z(r) \tag{6}$$

In Eq. (6), the integrations over $z$ and $r$ are both over the entire downstream domain. By combining Eqs. (1) and (6), the effective $\langle l_\Omega \rangle$ can be obtained for any given beam profile.

## III. Effects of Beam Shape and Plume Divergence

As an illustration, we now carry out sample calculations of the effective charge-exchange length for some hypothetical beam profiles. For simplicity, we assume that the shape, but not the diameter, of the beam profile is independent of the axial coordinate $z$. Thus, the radial beam profile can be expressed as a function of a scaled radial coordinate $\rho \equiv r/R_z$ (see Fig. 1). Formally, this dimensionless radial profile can be defined as

$$P(\rho) = \begin{cases} R_z^2 J_z(\rho R_z)/J_b, & \rho \leq 1, \\ 0, & \text{otherwise} \end{cases} \tag{7}$$

This profile is normalized so that

$$\int_0^\infty P(\rho)\rho\,d\rho = 1 \tag{8}$$

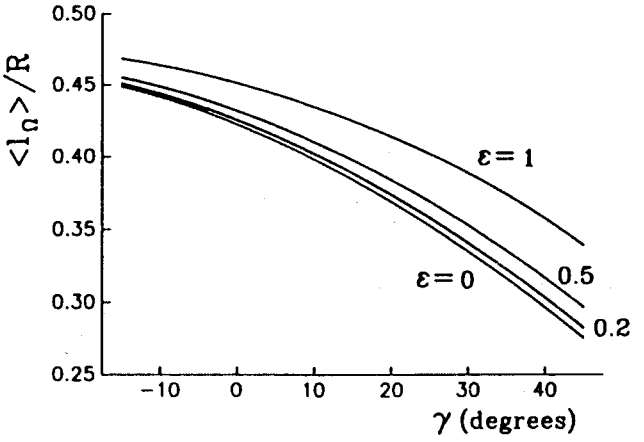


**Fig. 3 Effective $\langle l_\Omega \rangle$ (in units of the thruster radius $R$) as a function of $\gamma$ from Fig. 1 and $\varepsilon$ from Eq. (11).**

We assume, furthermore, that $R_z$ is given by a linear expansion of the beam, so that

$$R_z = R + z \tan \gamma \tag{9}$$

(negative values of $\gamma$ correspond to a converging beam, see Fig. 1).

Combining Eqs. (1), (6), (7), and (9), an expression for $\langle l_\Omega \rangle$ is obtained in the form of a fourfold integral. The integral over $z$ can be performed analytically, yielding

$$\langle l_\Omega \rangle = \frac{R}{\pi} \int_0^\pi d\varphi \int_0^1 \int_0^1 \frac{P(\rho)\rho \, d\rho\sigma \, d\sigma}{A\sqrt{C} + B\sqrt{A}} \tag{10a}$$

where

$$A = 1 + \rho^2 \tan^2\gamma \tag{10b}$$

$$B = \rho \tan \gamma(\rho - \sigma \cos \varphi) \tag{10c}$$

$$C = \rho^2 + \sigma^2 - 2\rho\sigma \cos \varphi \tag{10d}$$

and $\sigma \equiv s/R$ is the reduced radial coordinate in the thruster plane. For a nondiverging plume ($\gamma = 0$), it is possible to carry out one further integral analytically (either that over $\rho$ or that over $\sigma$). Beyond this, calculation of $\langle l_\Omega \rangle$ must proceed by numerical means.

Figure 3 shows calculated values of $\langle l_\Omega \rangle / R$ as a function of $\gamma$ for some parabolic beam profiles, which are defined as

$$P(\rho) = [4/(2 - \varepsilon)](1 - \varepsilon\rho^2), \qquad \rho \leq 1 \tag{11}$$

The parameter $\varepsilon$ in Eq. (11) determines the deviation from a flat profile. For a flat beam ($\varepsilon = 0$) and a divergence half-angle of 10 deg, the effective charge-exchange length is about $0.40R$. The inverse correlation between charge-exchange length and divergence half-angle in Fig. 3 is easily understood by inspection of Fig. 2: as the beam fans out, more charge-exchange collisions take place in regions with a lower solid-angle-probability of reaching the grid.

The largest possible value of $\langle l_\Omega \rangle$ is $0.5R$. This limit is reached for a beam profile that is concentrated entirely on the axis, with $P(\rho) > 0$ only for $\rho = 0$. This case may be approximated by a low-divergence beam from a thruster with a single aperture, whose diameter is much smaller than that of the grid in which it is embedded.

## IV. Nonuniformity of Grid Erosion

Among the strengths of the PIC codes are that they are capable of calculating how erosion is distributed around individual grid apertures, for example, in the case of pitting. However, because PIC codes are single-aperture in nature, they do not readily provide an insight into how the erosion is distributed across the diameter of the grid. Some insight, within the bound of the assumptions stated in Sec. II, is easily obtained from the present model. All that needs to be changed from the procedure employed in Secs. II and III is that the integration over the radial thruster coordinate $s$ or $\sigma$ not be performed. Carrying out the integrations over the remaining variables, the impingement current is obtained as a function of the radial position on the grid. To first approximation, this distribution of impingement current may be taken to be indicative of the distribution of grid erosion. (A more detailed calculation would have to incorporate the dependence of the sputter yield on the energy and angle of incidence of the CE ions, and the effect of redeposition of sputtered material.)

As an illustration, calculations were performed for beam profiles from Eq. (11) with $\varepsilon = 0$ (a flat profile) and $\varepsilon = 0.2$. The results are shown in Fig. 4 for different values of $\gamma$. Clearly, the maximum impingement current (and presumably, the maximum erosion) takes place at the center of the thruster. This is purely a geometric effect associated with the distribution of solid-angle-probabilities shown in Fig. 2. Toward the edges, fewer CE ions are collected, and the impingement current and erosion rate drop off. This effect is particularly strong for a nondiverging beam, as follows from the curve with $\gamma = 0$ in Fig. 4. As the beam divergence increases, the beam spreads out over a larger region, resulting in a more uniform erosion pattern.

## V. Comparison with Experiment

We now check our model against experimental data for two widely different tests. Case 1 refers to data collected by the

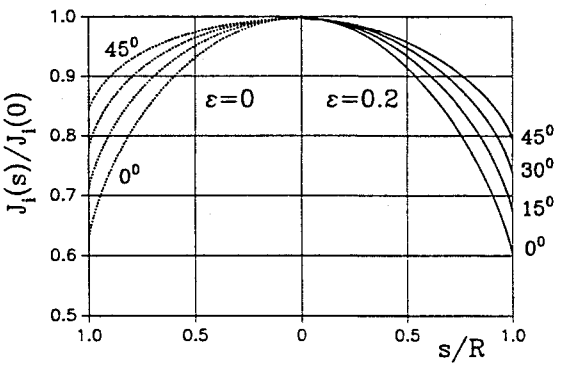


**Fig. 4 Radial variation of the impingement current on the accelerator grid for a flat beam ($\varepsilon = 0$) and a beam with a flatness parameter of 80% ($\varepsilon = 0.2$). Data are normalized to unity at the center of the grid. Curves correspond to different values of $\gamma$.**

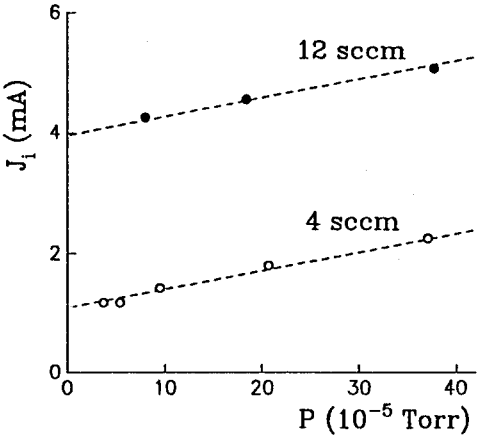


**Fig. 5 Measured impingement current as a function of chamber pressure for case 1 from Table 1 at total flow rates of 4 and 12 sccm.**

**Table 1 Comparison of predicted and measured ratios of impingement current to beam current for two tests**

| Case | $n_0$, $10^{17}$ m$^{-3}$ | $\sigma_{ce}$, $10^{-20}$ m$^2$ | $\gamma$, deg | $\varepsilon$ | $\langle l_\Omega \rangle / R$ | $2R$, cm | $(J_i/J_b)_{pred}$, % | $(J_i/J_b)_{exp}$, % |
|---|---|---|---|---|---|---|---|---|
| 1 | 32[a] | 21.2[b] | 15 | 0.5[d] | 0.45[e] | 3.8[f] | 0.58 | 0.69 ± 0.04[g] |
| 2 | 4.5[a] | 32.3[c] | 10 | 0.20 | 0.40 | 28.2 | 0.82 | 0.55 |

[a]Calculated from pressure assuming a gas temperature of 300 K.
[b]From Ref. 6 (p. 416) for argon at a beam energy of 550 eV.
[c]From Ref. 6 (p. 416) for xenon at a beam energy of 1517 eV.
[d]Defined at $2r = 3.0$ cm.
[e]Corrected for the fact that the exposed diameter of the grid is larger than the net beam diameter.
[f]Exposed diameter of the grid; the beam diameter is only 3.0 cm.
[g]Net chamber contribution at a pressure of $10^{-4}$ torr.

author on a commercial 3-cm ion source operating on argon.[7] Case 2 refers to a test of a 30-cm ion thruster at NASA Lewis Research Center operating on xenon.[8] Table 1 summarizes the results. Values of $\gamma$, $\varepsilon$, and $\langle l_\Omega \rangle$ are estimates. On the far right, the predicted and measured values of the ratio of impingement and beam currents are given.

For case 1, CE ions from neutral gas leaking out of the source may be expected to account for a large part of the measured impingement current because of the low ionization efficiency of the source (<25%). To isolate the effect of the chamber gas, the impingement current was measured as a function of the chamber pressure, while keeping the beam current (45 mA) and total flow rate (either 4 or 12 sccm) constant. Figure 5 shows the results. Simultaneous linear fits for both flow rates (dashed lines in Fig. 5) yield a slope of 0.31 ±0.02 mA per $10^{-4}$ torr. In Table 1 this chamber contribution is stated as a net chamber-induced $J_i/J_b$ ratio (0.69 ± 0.04%) at a pressure of $10^{-4}$ torr. The predicted value for the same conditions (0.58%) was calculated based on the exposed diameter of the grid (3.8 cm), which is considerably larger than the net diameter of the beam (3.0 cm). Considering the crudeness of both the geometric model and the experiment, the agreement between the predicted and measured values of $J_i/J_b$ seems quite reasonable.

For case 2, the ratio $J_i/J_b$ in Table 1 is taken directly from Ref. 8; no attempt was made to isolate the effect of backstreaming of CE ions from the chamber. Therefore the predicted value of $J_i/J_b$ (0.82%) should be low, having neglected any contributions from CE ions generated near the grids or from CE ions arising from the small fraction of neutral atoms (≃10%) that leak from the thruster. However, the predicted value is 50 percent higher than the measured value. The most obvious interpretation of this result is that, unlike assumed in Sec. II, CE ions produced in the plume are somehow prevented from backstreaming to the accelerator grid. Our simple model does not suggest a detailed mechanism for such shielding, which could be due either to the existence of an effective potential barrier just upstream of the neutralization plane, or to the existence of small radial potential gradients in the quasi-neutral region of the plume (the possibility of which was suggested by one of the reviewers).

## VI. Discussion and Conclusions

The simple geometric model presented here should be particularly useful for obtaining a quick estimate of the effect of backstreaming of CE ions from the chamber to the accelerator grid of a two-grid ion thruster. For this purpose, Eq. (5) may be used with a typical value of $\langle l_\Omega \rangle = 0.4R$. For a more refined estimate, $\langle l_\Omega \rangle$ can easily be computed for a given beam shape and divergence angle by numerical integration of Eqs. (10). The resulting value can be used, for example, to set the boundary condition for a single-aperture PIC calculation with regard to backstreaming of CE ions from the chamber. This would be an improvement over the approach employed in Ref. 3, in which the downstream boundary condition is chosen to match the measured impingement current, thereby compromising the predictive capability of the code.

The geometric model is crude, especially with regard to the assumptions that CE ions from the plume are not prevented from backstreaming to the accelerator grid by potential gradients close to the grid, or by radial potential gradients that may exist in the plume. In the case of a potential hill close to the grid, the PIC code would still benefit from having an independent way of setting the downstream boundary condition with respect to the backstreaming of CE ions from the chamber; more so because the formation of any potential hill that prevents CE ions reaching the grid may depend strongly on the magnitude of the flux of CE ions that backstream from the plume. If radial potential gradients in the plume prevent ions from backstreaming to the thruster, PIC codes may be in no better position to model the effect, because of their single aperture nature.

In conclusion, a simple geometric model has been discussed that may be used to estimate the impingement current on the accelerator grid of a two-grid ion thruster that results from backstreaming of charge-exchange ions from the plume. Among the potential uses of the model is to aid in setting the downstream boundary conditions for single-aperture-based particle-in-cell calculations.

## Acknowledgments

Funding for this work was provided by NASA Grant NAGW-1195, and by Boeing Defense and Space Group of Seattle, Washington. The concept of a solid-angle-based calculation of the impingement current on a thruster grid is based in part on previous work by the author (see the last four paragraphs of Sec. II-B of Ref. 1). However, the more direct impetus for the present work was provided by a similar concept that has been proposed independently by P. Wilbur and J. Monheiser of Colorado State University. I gratefully acknowledge their sharing their work freely. Finally, I appreciate discussions with X. Peng.

## References

[1]Peng, X., Ruyten, W. M., and Keefer, D., "Plasma Particle Simulation of Electrostatic Ion Thrusters," *Journal of Propulsion and Power*, Vol. 8, No. 2, 1992, pp. 361–366.

[2]Peng, X., Ruyten, W. M., Friedly, V. J., Keefer, D., and Zhang, Q., "Particle Simulation of Ion Optics and Grid Erosion for Two-Grid and Three-Grid Systems," *Review of Scientific Instruments*, Vol. 65, No. 5, 1994, pp. 1770–1773.

[3]Peng, X., Ruyten, W. M., and Keefer, D., "Further Study of the Effect of the Downstream Boundary Condition on Accelerator Grid Erosion in an Ion Thruster," AIAA Paper 92-3829, July 1992.

[4]Monheiser, J. M., and Wilbur, P. J., "An Experimental Study of Impingement-Ion-Production Mechanisms," AIAA Paper 92-3826, July 1992.

[5]Lathem, W. C., "Ion Accelerator Designs for Kaufman Thrusters," AIAA Paper 69-261, March 1969.

[6]Hasted, J. B., *Physics of Atomic Collisions*, Butterworths, London, 1964, p. 413.

[7]Ruyten, W. M., Friedly, V. J., Peng, X., Celenza, J. A., and Keefer, D., "Spectroscopic Investigations of Beam-Plasma Interactions in an Ion Plume," AIAA Paper 93-1791, June 1993.

[8]Patterson, M. J., and Verhey, T. R., "5 kW Xenon Ion Thruster Life Test," AIAA Paper 90-2543, July 1990.